Journal of Biomedical Optics 7(3), 313–320 (July 2002)

Analysis of the spatial distribution of polarized light backscattered from layered scattering media

I. M. Stockford
S. P. Morgan
P. C. Y. Chang
J. G. Walker
University of Nottingham
School of Electrical and Electronic Engineering
University Park
Nottingham NG7 2RD
United Kingdom

Abstract. The scattering of polarized light from a two layer scattering medium is investigated using Monte Carlo simulations. First order and normalized second order moments are used to analyze the spatial properties of the emerging light in different polarization states. Linearly and circularly polarized illumination is used to probe different depths. Absorption and layer thickness are varied and it is demonstrated that the determination of these values is aided by the inclusion of polarization information. The lateral and depth localization of light by polarization subtraction is also quantified. Potential applications of these techniques are burn depth and melanoma thickness measurements.
[DOI: 10.1117/1.1483316]

Keywords: polarization; Mie scattering; layer thickness; Monte Carlo.

Paper TP-07 received July 31, 2001; revised manuscript received Dec. 7, 2001; accepted for publication Dec. 21, 2001.

1 Introduction

Much effort has been directed towards the development of noninvasive optical techniques to interrogate the human body for medical purposes.[1] These techniques provide fast diagnosis with minimal discomfort to the patient and disruption to the area of interest. The main drawback is that light is heavily scattered within tissue and this leads to uncertainty in the volume from which information is retrieved. There is an increasing interest in the use of optical techniques for characterizing layered media for applications such as burn depth measurement and melanoma diagnosis. In burn applications, depth is the most important parameter to clinicians when diagnosing the need to perform a skin graft,[2] e.g., a deep second degree burn penetrates into the dermis to a depth of the order of 1–2 mm.[3] Depth is also important in melanoma diagnosis, as the cancer may spread if the epidermis/dermis boundary is broken.[4]

Several techniques have been applied to analyze layered scattering media. Time of flight[5,6] and diffusive wave analysis[7,8] have shown potential for relatively thick layers ($\sim$several mm). Optical coherence tomography[9] and confocal microscopy[10] have been used to image thinner layers ($<500\ \mu$m). Polarization techniques can also be employed to image scattering media[11–16] and are advantageous as the systems are relatively simple, allowing measurements to be made by unskilled operators in a short time period. Polarized light techniques utilize the property that light depolarizes as it propagates[17] and the initial polarization of incident light is lost within relatively few scattering events. This can be used to localize volumes close to the surface. In addition, it has been observed that there are varying rates of depolarization of different initial polarization states with scattering[18] and suggested[19] that this can be used to characterize layered scattering media and perform coarse optical sectioning. The spatial distribution of light backscattered from a multilayered medium[20] has also been shown to possess depth discrimination properties. The greater the distance of light emergence from the input source position the higher the probability of probing deeper. This study uses a layered polarization Monte Carlo model to investigate whether a combination of polarization and spatial techniques will lead to improved characterization of layered media.

In the following section the analysis methods used in the study are presented, including the specifics of the Monte Carlo simulation, the samples under consideration and the regimes used to perform polarization discrimination. In Sec. 3 results are presented investigating the spatial distributions in different polarization channels for media with different properties. Discussions and conclusions follow in Secs. 4 and 5.

2 Theory

2.1 Monte Carlo Simulation

The polarization Monte Carlo model simulates illumination with a pencil beam of polarized light perpendicular to its surface and models individual photons (or light packets) propagating through a layered scattering medium composed of Mie scattering particles.[21] The details of this model have been discussed previously[22,23] and is, therefore, addressed only briefly here. Photons are individually tracked through the medium and at each photon-particle collision the direction and polarization are modified, via adjustment of the directional cosines and Stokes parameters. The characteristics of photons backscattered from the medium are recorded. Spatial intensity distributions, $I(r)$, are obtained by measuring the frequency of photons emerging within annuli centered on the source and normalized by the annular area. All results presented are for a bin size of 0.25 mean free paths (MFP$=1/\mu_s$).

Address all correspondence to Steve Morgan. Tel: +44-115-9515570; Fax: +44-115-9515616; E-mail: steve.morgan@nottingham.ac.uk

1083-3668/2002/$15.00 © 2002 SPIE

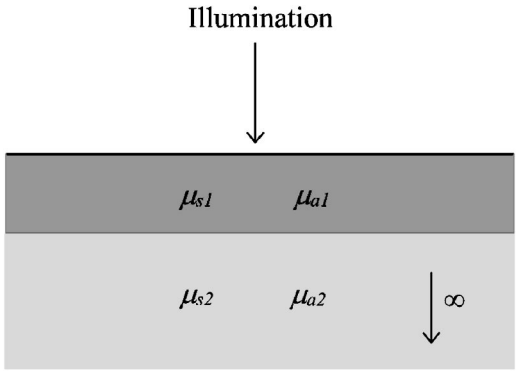

Fig. 1 General sample geometry.

2.2 Samples and Sample Geometries

Figure 1 shows the general form of the sample under investigation. The model is capable of simulating multiple layers each infinite in the $x-y$ plane with a semi-infinite lower layer. However, for simplicity we consider a two layer medium in this study, with an upper planar layer and a semi-infinite lower layer. There is a mismatch of 1.4 in the refractive index at the air-tissue interface and at the tissue–tissue interface the layers are considered to be index matched. The medium is comprised of a monodispersion of Mie scatterers with the mean cosine of the scattering angle, $g=0.92$ and size parameter $ka=13.9$, and are consistent with typical tissue scatterers.[1] Each layer has different scattering (μ_s) and absorption (μ_a) coefficients and absorption is added postsimulation using Lambert–Beer's law, depending on the propagation distance within each layer. The absorption and scattering properties of the media analyzed are stated in MFPs so that the results can be easily scaled for a wide range of media.

2.3 Polarization Analysis

Light of different initial polarization states can be used to obtain sensitivity to different depths within the layered medium.[19] The technique relies on the property that different illuminating polarization states depolarize at different rates on propagation through the medium. The ability of a photon to maintain its polarization is dependent on the shape, size and material properties of scattering particles encountered and this has been explored extensively elsewhere.[9,18,21,24] For the particles considered in this investigation, light that is initially linearly polarized maintains its polarization for fewer scattering events than for circularly polarized illumination.

To utilize these properties, a four channel detection scheme is used with different illumination and detection arrangements (Table 1). These channels can be easily measured experimentally using a simple detection scheme.[15,19] The different channels allow various categories of backscattered photons to be detected (Figure 2). Considering the linear case [Figure 2(a)], there are two categories of backscattered light. The first is light that has undergone relatively few scattering events and maintains its initial polarization, and has thus propagated close to the surface of the medium. The second is light that has traveled a greater distance and emerges with random polarization, thus contributing equally to channels 1 and 2.

For circularly polarized light, three categories of emerging light can be defined. The first is that which is almost immediately backscattered upon entering the scattering medium. This mirror reflection results in a flip in helicity of the incoming circular polarization and contributes to the orthogonal circularly polarized channel 4. The second category is that which has undergone a series of forward scattering events and emerges from the medium having maintained its initial polarization state. As the particles considered here are heavily forward scattering, there is a significant contribution from this second category to channel 3. Finally, photons that have random polarization through multiple scattering contribute equally to channels 3 and 4. The different categories of polarized light have different penetration depths (Figure 2) and so can potentially be used to characterize layered media. The detected channels can be used to define the degree of polarization (DOP) of the backscattered light with respect to its initial polarization. In the case of the linear illumination, this is defined as

$$\mathrm{DOP}_L=\frac{I_1-I_2}{I_1+I_2}, \tag{1}$$

where I_1 and I_2 represent the backscattered intensity in channels 1 and 2, respectively. The circular equivalent replaces I_1 and I_2 by the channel 3 and 4 intensities, I_3 and I_4, respectively.

2.4 Moments of Distributions

Moment analysis is a widely used technique for curve analysis and provides a useful method of characterizing the spatial

Table 1 Polarization discriminating detection schemes.

Channel	Illumination	Detection	Categories of light
1	Linear (horizontal)	Linear (horizontal)	Polarization maintaining and multiply scattered light
2	Linear (horizontal)	Linear (vertical)	Multiply scattered light
3	Circular (right)	Circular (right)	Forward scattered and multiply scattered light
4	Circular (right)	Circular (left)	Mirror reflected and multiply scattered light

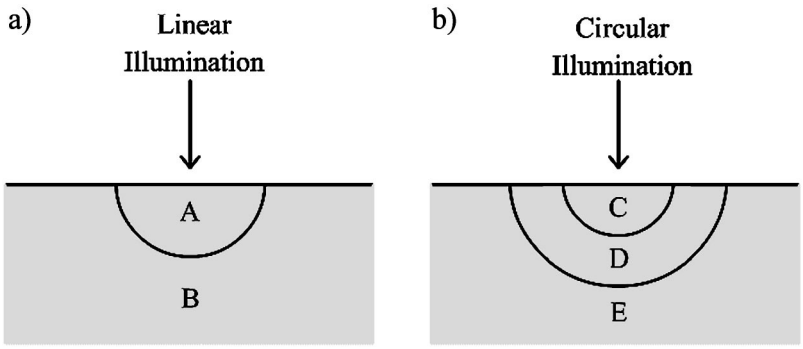

Fig. 2 Photon categories emerging from the surface of a scattering a medium. (a) Linearly polarized illumination showing the visitation region of polarization maintaining light (A) and random polarization (B). (b) Circularly polarized illumination showing the regions probed by mirror reflected light (C), polarization maintaining light (D) and randomly polarized light (E).

intensity distributions obtained in this study. The first order moment, M_1, and normalized second order moment, N_2, are defined as

$$M_1 = \int_{r=0}^{\infty} P(r) r dr, \tag{2}$$

$$N_2 = \frac{\int_{r=0}^{\infty} P(r) r^2 dr}{M_1^2}, \tag{3}$$

where $P(r)$ is a probability density function estimated by normalizing the area under the photon frequency histogram $I(r)$ to unity [$I(r)$ is obtained by the procedure described in Sec. 2.1]. M_1 represents a measure of the width of the distribution and N_2 is characteristic of the shape of the distribution, more heavily influenced by photons measured further from the source.

3 Results

To determine the general properties of the intensity distributions it is instructive to first consider a semi-infinite homogeneous medium. An analysis of the spatial distributions in polarization channels 1–4 for a semi-infinite homogeneous medium are presented in Sec. 3.1, including the subtraction of these channels to enable localization of different volumes. These concepts are then extended to the analysis of a two layer medium in Sec. 3.2 for different values of absorption and layer thickness.

3.1 Semi-Infinite Homogeneous Medium

Figure 3 shows the spatial intensity and spatial DOP distributions for a semi-infinite homogeneous medium with unity MFP and zero absorption. Considering first the linear channels, it can be seen that, for radial distances up to 15 MFPs from the source, channel 1 is greater in intensity than channel 2. As discussed in Sec. 2.3, both channels contain equal amounts of multiple scattered light but channel 1 contains an additional component that has maintained the original polarization. At high radial distances there is no polarization maintaining light and so the DOP tends to zero [Figure 3(b)]. It is interesting to note that the peak in the linear DOP is positioned away from the source ($r = 0.5$ MFPs). At positions close to the source there is a high proportion of singly scattered photons that exhibit Mie scattering properties, e.g., in the bin nearest the source 40% of the photons are singly scattered. The detailed structure of the Mie scattering footprint contributes to a variation in intensity in the co- and cross channels with detector position which, when averaged over the detection bins, results in a higher DOP away from the source. This effect arises as we have used a single particle size in the simulation. In practice for tissue scattering, where there

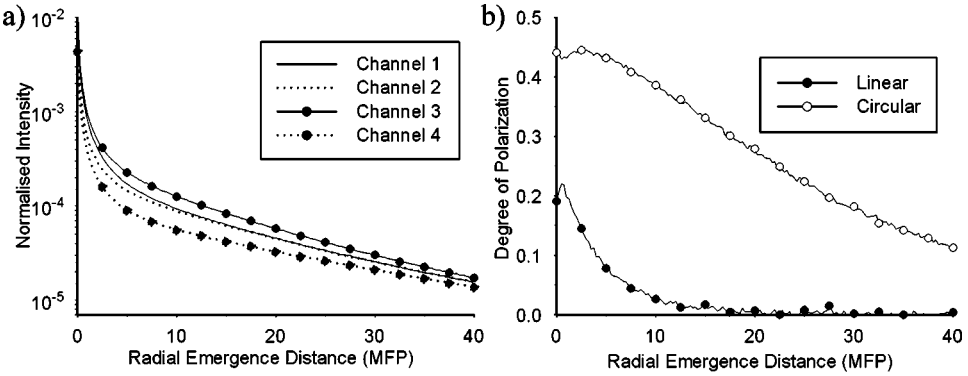

Fig. 3 (a) Backscattered intensity spatial distributions in the four illumination and detection regimes and (b) the resulting spatial DOP distribution for linearly and circularly polarized illuminations.

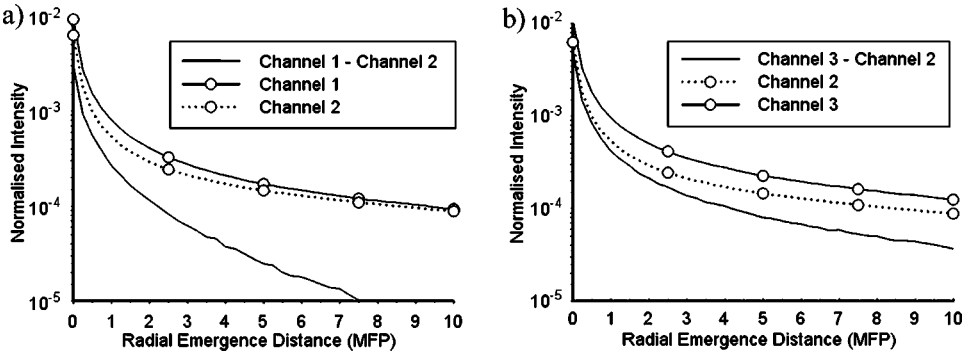

Fig. 4 Lateral localization obtained by extracting (a) linear polarization maintaining light (ch1-ch2), (b) circular polarization maintaining light (ch3-ch2).

is a range of particle sizes, it is unlikely that this feature will be observed. A simple subtraction of these two channels retrieves light that has probed only a shallow depth. This technique has been used previously to remove multiple scattered light and improve image quality of structures within scattering media[11,13,14,16] Figure 4(a) demonstrates how subtraction of linear polarization channels enables lateral localization to be obtained. The subtraction reduces the tail of the distribution due to elimination of scattered light. However, this has negligible effect on the 1/*e* width of the distributions due to the high intensity close to the source.

Figure 3(a) shows a difference between channels 3 and 4 for all radial positions considered, resulting in a significantly higher circular DOP compared to linear [Figure 3(b)]. This confirms the greater ability for circularly polarized light to maintain its polarization. The peak in the DOP is away from the source ($r=2.75$) as there is a contribution from the mirror reflected light to the cross-polar channel 4 at the source. Circular polarization maintaining photons can also be extracted using subtraction techniques as shown in Figure 4(b), again reducing the tail of the distribution. The circular polarization maintaining light emerges at a greater radial distance from the source than linear polarization maintaining light suggesting that it has probed a deeper level. This is confirmed by plotting the maximum photon visitation depth (normalized to peak intensity in channel) for linear and circular polarization maintaining light extracted by calculating I_1-I_2 and I_3-I_2, respectively (Figure 5). (I_2-I_3 assumes that the amount of depolarized light is the same in both linear and circular channels. This is not strictly true for pathlengths ~ 1 transport MFP due to the different polarization memory. However, it successfully enables the elimination of heavily scattered light as shown in Figure 5 and so provides a reasonable approximation.) Also plotted for reference is the maximum photon visitation depth for multiple scattered light (channel 2). This clearly shows that the extraction of different maintained polarizations provides interrogation of different depths, with the peak in the linear maintaining distribution occurring at 2 MFPs into the sample and 7 MFPs for the circularly polarized maintaining illumination, compared with a peak at 10 MFPs for the multiple scattered light. This property suggests that different polarizations can be used to characterize different layers within the medium.

3.2 Layered Media

Before considering medium absorption and layer thickness it is useful to demonstrate the general properties of the intensity distributions of layered media. Initially a two layer medium with top and bottom MFPs of 1.0 and 2.0, respectively, is considered. Both layers have zero absorption, the top layer is 10 MFPs thick (all measurements of absorption and layer thickness are relative to the top layer MFP) and the bottom layer is semi-infinite. Figure 6 shows the spatial intensity distributions of the four polarization channels, superimposed with the response of a semi-infinite homogeneous medium with the same properties as the individual layers. All channels show that at low radial distances (typically $r<4$ MFPs) the spatial response of the two layer medium follows that of a semi-infinite homogeneous medium with the properties of the top layer. Conversely, further from the source (typically $r>30$ MFPs), the intensity distribution tends towards that of a semi-infinite homogeneous medium with the properties of the second layer, confirming the interdependence of depth and radial emergence distance. Another observation that can be made from these plots is that channel 4 tends toward the response of the second layer at a slower rate than channel 3. This subtle difference is due to channel 4 containing a light component that has propagated a shorter distance and is there-

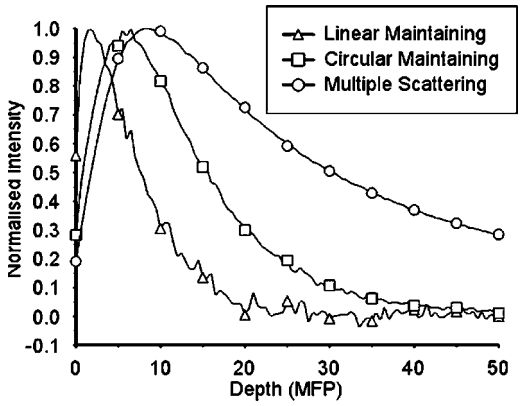

Fig. 5 Visitation depth of polarization maintaining illumination for linearly maintaining, circularly maintaining and multiple scattered light.

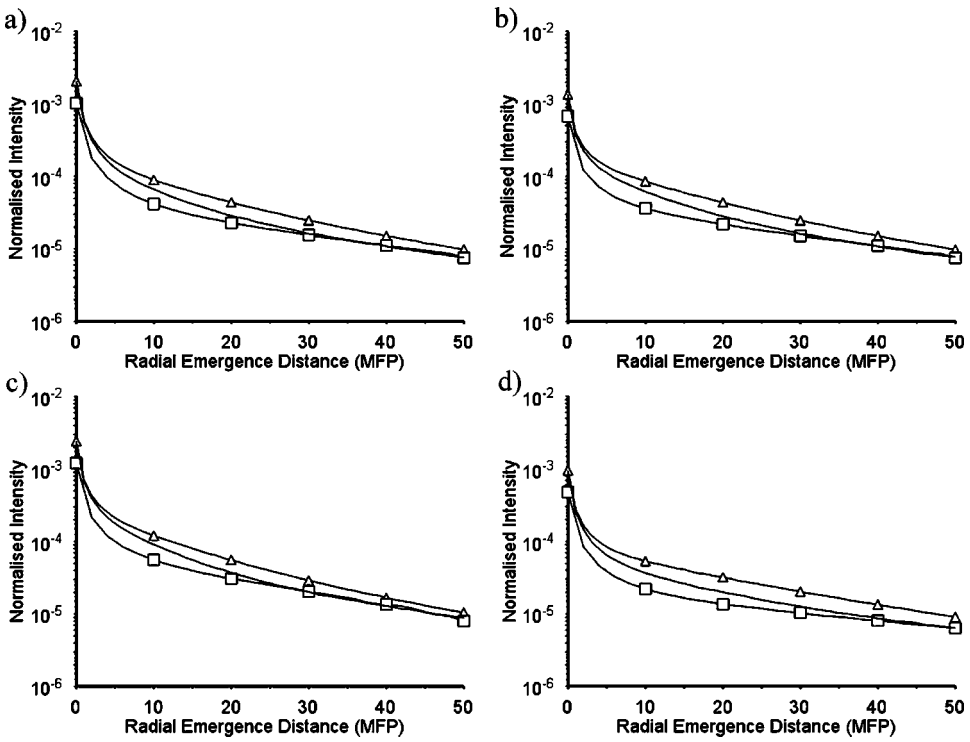

Fig. 6 Spatial intensity variations for a two layer medium (solid line) with a top layer MFP of unity, bottom layer MFP of 2.0, top layer thickness of 10.0 MFPs and zero absorption in (a) channel 1, (b) channel 2, (c) channel 3, (d) channel 4. Superimposed on the curves are measurements for semi-infinite media with optical properties of the top layer (-△- line) and lower layer (-□- line).

fore more representative of the top layer. Having demonstrated the dependence of the distributions on the two layers, the absorption and layer thickness is considered.

3.2.1 *Layer Thickness*

Using an approach described previously[19] we have modeled layer thickness using a single layer medium. This is equivalent to an upper layer with varying thickness above a second layer that is totally absorbing. The advantage of this approach is that a single Monte Carlo simulation can be used to model different layer thickness by recording the maximum visitation depth of a photon and discarding those absorbed in the second medium. This improves the efficiency of the simulations and enables sufficient photons to be obtained to calculate the moments of subtracted distributions. However, it should be noted that this represents the extreme contrast for a two layer medium.

Figures 7(a) and 7(b) show the first and normalized second order moments for the four polarization channels. All channels demonstrate a sensitivity to layer thickness and some differences are observable between the channels containing polarization maintaining light (1 and 3) and channels 2 and 4. These differences are relatively small as the channels contain a common multiple scattered background. Figures 7(c) and 7(d) show the first and normalized second order moments for extracted linearly and circularly polarized light and those of multiple scattered light (channel 2) for reference. As demonstrated in Figure 5 the majority of linearly and circularly polarized light is maintained within the top 15 and 30 MFPs, respectively, and so the moment calculations are insensitive to thicker layers. The elimination of multiple scattered light enhances the differences between the moments of these cases and potentially may be better conditioned for inversion.

When the two layer model is used to simulate layer thickness the differences between the polarization channels reduces due to a high contribution of multiple scattered light from the lower layer. It would be useful to measure the moments of the distributions from the polarization maintaining light over the range of thickness for a two layer model. Under these conditions the elimination of multiple scattered light should provide a greater sensitivity to layer thickness and the results should have comparable sensitivity to Figures 7(c) and 7(d). At present this is impractical due to long computation time and an accelerated Monte Carlo[23] is a more viable option.

3.2.2 *Layer Absorption*

Absorption is also an important consideration due to factors such as the melanin content of the upper layer and blood concentration of underlying layers. In this section the MFP of both layers was set to unity to remove any influence due to a scattering mismatch between layers. The top layer thickness is fixed at 10 MFPs and the top and bottom layer absorption is varied. The first and normalized second order moments of the different polarization channels are presented in Figure 8 using contour plots to show variation with absorption of both layers. Featured on these plots are lines of constant first order (solid) and normalized second order moments (dashed) with variation of absorption in the top and bottom layers. It can be seen from these that if both the first and normalized second order moments are known the absorption of the two separate layers

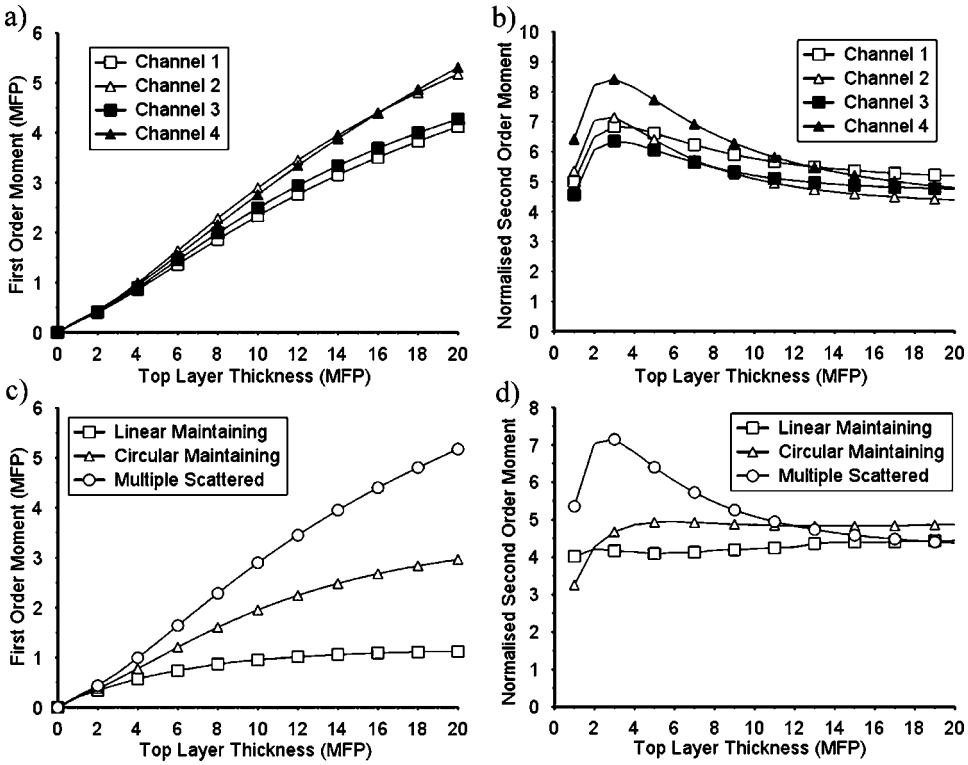

Fig. 7 Top layer thickness variation (top layer MFP = 1.0, absorption = 0, bottom layer absorption = ∞). (a) First order moment of channels 1–4, (b) normalized second order moment of channels 1–4, (c) first order moment of extracted linear (ch1-ch2) and circular (ch3-ch2) polarization states, (d) normalized second order moment of extracted polarization states.

can be determined. Practical application of such a technique indicates that the more perpendicular the two sets of contours, the lower the sensitivity to noise on either value.[25]

The first observation is that the first order moment is heavily dependent on the characteristics of the top layer. This can be seen from the contours being nearly vertical, hence a variation in bottom layer absorption results in a small change in first order moment, but a top layer alteration produces a significant change in this parameter. Another feature that confirms this dependence is that the first order contours are steeper in channels 1 and 4 than in 2 and 3 as these channels are more dependent on the top layer. The second order moment is heavily influenced by light emerging further from the source [Eq. (3)] and so is more dependent on the characteristics of the second layer, resulting in more horizontal contours.

4 Discussion

The results have demonstrated the potential of using the spatial distribution of polarized light for characterizing layered media. It has been shown that lateral localization can be obtained by subtracting different polarization states (Figure 4). The difference in probing depth of different polarization states can be used to extract information from distinct regions within the sample. This has been confirmed in Figure 5 showing a clear difference in visitation depth between multiple scattered, linear and circular polarization maintaining photons. If a MFP of 100 μm in skin is assumed,[1] the peaks in the depth distributions correspond to 200 and 700 μm for linear and circular, respectively, and 1 mm for the multiple scattered light. The spatial position of emergence also provides sensitivity to different layers, with light emerging further from the source more heavily influenced by the lower layer. This is also evident in the moment analysis (Figure 8) as the second order, which is influenced by larger positions of emergence, depends more on the lower layer.

The results presented in this paper have demonstrated the dependence of the spatial distribution of polarized light on the optical properties and layer thickness of a layered scattering medium. Ideally one would like to be able to make sufficient optical measurements to extract layer thickness and the scattering and absorption properties of both layers. The measurements proposed here offer a potential method of achieving this, however inverting the data to obtain these five parameters is a difficult problem. We are currently training a neural network to investigate whether this is feasible and whether data obtained from subtracted data are better conditioned than those from the individual channels. It may be necessary to assume the optical properties of the layers from published data[1] to extract information about layer thickness. Alternatively, for the two layer medium considered in this study it is clear that linear polarization maintaining light can be used to measure the optical properties of the top layer more or less independently of the underlying layer. These could then be used in a three parameter inversion to obtain layer thickness and the properties of the lower layer.

When considering the results of a theoretical study such as this it is necessary not to lose sight of the final experimental implementation. One factor in favor of polarization tech-

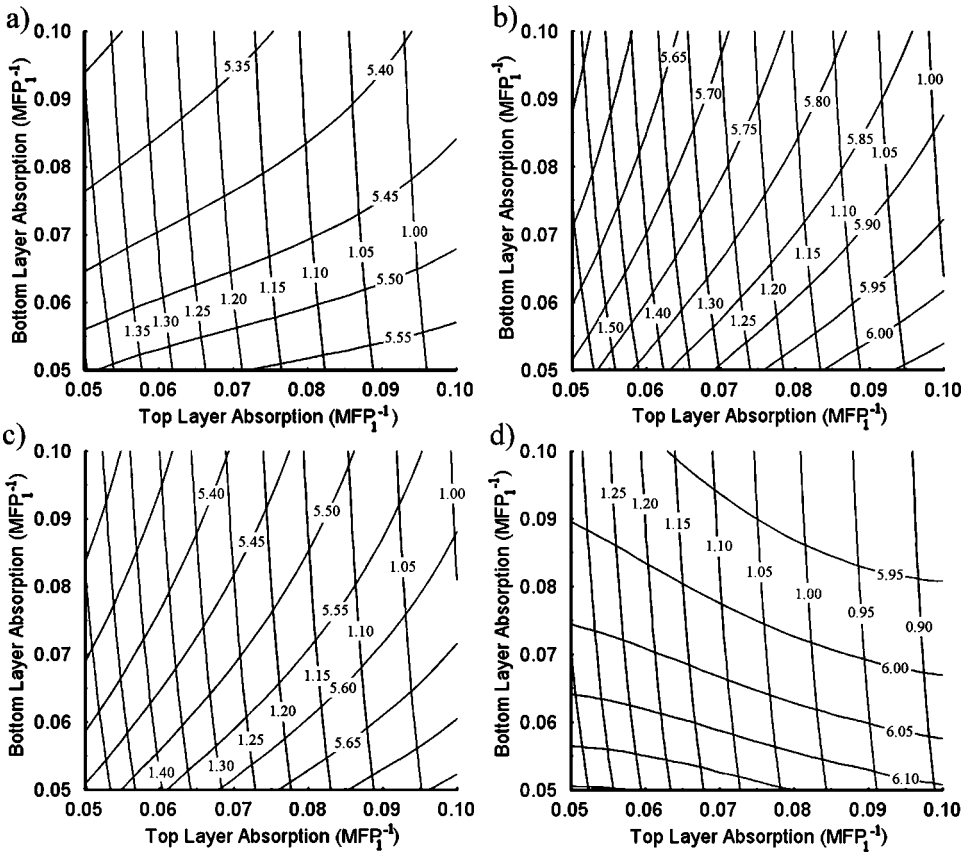

Fig. 8 Contour plots of the first (solid line) and normalized second order (dotted line) moments for different top and bottom layer absorptions in (a) channel 1, (b) channel 2, (c) channel 3 and (d) channel 4.

niques is that the instrumentation required is very simple, low cost and easily used by clinicians. In this study the main aim was to determine whether information about the medium under investigation could be obtained using polarized light measurements. Clearly this has been demonstrated but several effects need to be considered before the method can be used in practice. The skin is a multilayered media and to extract the properties of each layer will be a difficult problem. Two properties not considered in this study but which may increase the contrast are the small refractive index mismatch at the tissue–tissue interfaces and the birefringence of different layers, e.g., collagen. These could be incorporated as demonstrated in recent studies by Wang.[26] In addition, to reduce noise in the Monte Carlo simulation we have integrated over the azimuthal angle to obtain the intensity distributions. There is an azimuthal dependence on the linear polarization intensity distributions[21,27] and, although this does not affect the trends of the moment calculations, there will be increased contrast at particular azimuthal angles in the linear channels which may also aid inversion.

Further studies are required to determine whether the polarization memory properties used here still occur when the scatterers, such as cells within tissue, are nonspherical or have a range of sizes. This will be investigated by incorporating nonspherical scattering functions into the Monte Carlo code and by experimental studies on tissue. Clearly, when there are different values of g used in the simulation then the polarization memory effects will differ[18] and so these will need to be quantified over a range of g values. For instance, at a $g = 0.85$ the peaks in Figure 5 are positioned at 0.5 and 3 MFPs for linear and circular polarization, respectively. In addition, the finite source geometry that will be applied in practice will need to be incorporated by convolving the current results with this source geometry. One problem that arises from the analysis of samples in backscatter is specular reflection from the air/medium interface. This is an important consideration in the measurement of spatial intensity distributions as the large peak at the origin has a heavy weighting on the value of the first order moment. This in turn, through the normalization process, influences the value of the normalized second order moment and so an error in the evaluation of M_1 will propagate through. A simple method of avoiding specular reflections is to use a matching fluid, an approach applied effectively by Jacques[14] and routinely used in dermatoscopy.[28]

5 Conclusions

The backscattered spatial intensity distribution of polarized light has been investigated as a method for characterizing layered scattering media. It has been demonstrated that subtraction of different polarization states enables both lateral and depth localization to be obtained and that circular polarization can be used to probe deeper than linear. Thus different polarization states show sensitivity to different layers within the medium. Furthermore, the radial position of emergence exhibits its sensitivity to the depth, light emerging nearer to the source

is more sensitive to the upper layer, whereas light emerging further from the source is more sensitive to the lower layer. Moment analysis has been used to study two layer scattering media with varying physical dimensions and optical absorptions. This confirms that different polarization channels have varying sensitivity to the different layers within the medium due to the variation in volume probed.

Acknowledgments

I.M.S would like to thank the Engineering and Physical Sciences Research Council (UK) for a research studentship. S.P.M is supported by a EPSRC advanced fellowship.

References

1. V. Tuchin, *Tissue Optics*, SPIE, Bellingham, WA (2000).
2. M. A. Afromowitz, J. B. Callis, D. M. Heimbach, L. A. DeSoto, and M. K. Norton, ''Multispectral imaging of burn wounds: a new clinical instrument for evaluating burn depth,'' *IEEE Trans. Biomed. Eng.* **35**, 842–849 (1988).
3. U. F. Lever and G. Schaumburg-Lever, *Histopathology of the Skin*, Lippincott, Philadelphia (1990).
4. R. M. MacKie, ''Clinical recognition of early invasive malignant melonoma,'' *Br. Med. J.* **301**, 1005–1006 (1990).
5. A. H. Hielscher, H. Liu, B. Chance, F. K. Tittel, and S. Jacques, ''Time-resolved photon emission from layered turbid media,'' *Appl. Opt.* **35**, 719–728 (1996).
6. T. J. Farrell, M. S. Patterson, and M. Essenpreis, ''Influence of layered tissue architecture on estimates of tissue optical properties obtained from spatially resolved diffuse reflectometry,'' *Appl. Opt.* **37**, 1958–1972 (1998).
7. T. H. Pham, T. Spott, L. O. Svaasand, and B. J. Tromberg, ''Quantifying the properties of two-layer turbid media with frequency-domain reflectance,'' *Appl. Opt.* **39**, 4733–4745 (2000).
8. L. O. Svaasand, T. Spott, J. B. Fishkin, T. Pham, B. J. Tromberg, and M. W. Berns, ''Reflectance measurements of layered media with diffuse photon-density waves: a potential tool for evaluating deep burns and subcutaneous lesions,'' *Phys. Med. Biol.* **44**, 801–813 (1999).
9. J. Welzel, E. Lankenau, R. Birngruber, and R. Engelhardt, ''Optical coherence tomography of the human skin,'' *J. Am. Acad. Dermatol.* **37**, 958–963 (1997).
10. B. R. Masters and P. T. C. So, ''Confocal microscopy and multiphoton excitation microscopy of human skin in vivo,'' *Opt. Express* **8**, 2–10 (2001) (http://www.opticsexpress.org/oearchive/source/27001.htm).
11. S. P. Morgan, M. P. Khong, and M. G. Somekh, ''Effects of polarization state and scatterer concentration on optical imaging through scattering media,'' *Appl. Opt.* **36**, 1560–1565 (1997).
12. J. M. Schmitt, A. H. Gandjbakhche, and R. F. Bonner, ''Use of polarized light to discriminate short-path photons in a multiply scattering medium,'' *Appl. Opt.* **31**, 6535–6546 (1992).
13. S. G. Demos and R. R. Alfano, ''Optical polarization imaging,'' *Appl. Opt.* **36**, 150–155 (1997).
14. S. L. Jacques, J. R. Roman, and K. Lee, ''Imaging superficial tissues with polarized light,'' *Lasers Surg. Med.* **26**, 119–129 (2000).
15. G. D. Lewis, D. L. Jordan, and P. J. Roberts, ''Backscattering target detection in a turbid medium by polarization discrimination,'' *Appl. Opt.* **38**, 3937–3944 (1999).
16. J. G. Walker, P. C. Y. Chang, and K. I. Hopcraft, ''Visibility depth improvement in active polarization imaging in scattering media,'' *Appl. Opt.* **39**, 4933–4941 (2000).
17. D. Bicout and C. Brosseau, ''Multiply scattered waves through a spatially random medium: entropy production and depolarization,'' *J. Phys. I* **2**, 2047–2063 (1992).
18. F. C. MacKintosh, J. X. Zhu, D. J. Pine, and D. A. Weitz, ''Polarization memory of multiply scattered light,'' *Phys. Rev. B* **40**, 9342–9345 (1989).
19. S. P. Morgan and M. E. Ridgway, ''Polarization properties of light backscattered from a two layer scattering medium,'' *Opt. Express* **7**, 395–402 (2000).
20. I. V. Meglinsky and S. J. Matcher, ''Modelling the sampling volume for skin blood oxygenation measurements,'' *Med. Biol. Eng. Comput.* **39**, 44–50 (2001).
21. A. H. Hielscher, J. R. Mourant, and I. J. Bigio, ''Influence of particle size and concentration on the diffuse backscattering of polarized light from tissue phantoms and biological cell suspensions,'' *Appl. Opt.* **36**, 125–135 (1997).
22. P. C. Y. Chang, J. G. Walker, K. I. Hopcraft, B. Ablitt, and E. Jakeman, ''Polarization discrimination for active imaging in scattering media,'' *Opt. Commun.* **159**, 1–6 (1999).
23. K. Turpin, J. G. Walker, P. C. Y. Chang, K. I. Hopcraft, B. Ablitt, and E. Jakeman, ''The influence of particle size in active polarization imaging in scattering media,'' *Opt. Commun.* **168**, 325–335 (1999).
24. H. C. van de Hulst, *Light Scattering by Small Particles*, Dover, New York (1981).
25. S. F. Baker, J. G. Walker, and K. I. Hopcraft, ''Optimal extraction of optical coefficients from scattering media,'' *Opt. Commun.* **187**, 17–27 (2001).
26. X. Wang and L. V. Wang, ''Propagation of polarized light in birefringent turbid media: time-resolved simulations,'' *Opt. Express* **9**, 254–259 (2001) (http://www.opticsexpress.org/oearchive/source/34757.htm).
27. M. J. Rakovic, G. W. Kattawar, M. Mehrubeoglu, B. D. Cameron, L. V. Wang, S. Rastegar, and G. L. Cote, ''Light backscattering polarization patterns from turbid media: theory and experiment,'' *Appl. Opt.* **38**, 3399–3408 (1999).
28. W. Stolz, O. Braun-Falco, P. Bilek, M. Landthaler, and A. B. Cognetta, *Color Atlas of Dermatoscopy*, Blackwell Science, Boston (1993).